International Journal of Advanced Engineering Research and Science (IJAERS) *[Vol-3, Issue-10, Oct- 2016]*
https://dx.doi.org/10.22161/ijaers/310.22 *ISSN: 2349-6495(P) | 2456-1908(O)*

Experimental Evaluation of Electrolyte Flow Pattern in ECM Tool Using CFD Analysis

Gali Chiranjeevi Naidu, K Dharma Reddy, P V Ramaiah

Department of mechanical engineering, SV University College of engineering, Tirupati, Andhra Pradesh, India

Abstract — *In this present study, three dimensional flow pattern of Electrochemical Machining process has been simulated using Computational Fluid Dynamics (CFD) in L-shaped tool model. The ANSYS software is used for the design and analysis of a model. Different process parameters like volume fraction profile, velocity profile, pressure profile temperature profile and heat flux profile of electrolyte flow in the Inter Electrode Gap (IEG) etc. have been evaluated from the simulation using this model. The results indicated generation of hydrogen bubbles in which the turn reduced the volume fraction of brine depending upon the tool geometry. Reduced brine volume fraction led to reduction in MRR. As a result of hydrogen bubble formation, temperature towards the boundaries were increased rapidly as gaseous hydrogen bubbles possess sufficiently lower convective heat transfer coefficient as compared to liquid brine. For validating the simulation results, a set of experiments have been carried out on ECM by fabricating the tool geometry. The experimental results were analyzed by using MINITAB software.*

Keywords — CFD, ECM, Electrolyte, Flow pattern*.*

I. INTRODUCTION

Electrochemical machining (ECM) is one of the most potential un-conventional machining processes. The basic principle may be considered as the reverse of electroplating with some modifications. Further, it is based on the principle of electrolysis. In a metal, electricity is conducted by the free electrons, but it has been established that in an electrolyte the conduction of electricity is achieved through the movement of ions. Thus, the flow of current through an electrolyte is always accompanied by the movement of matter. Thus ECM can be thought of a controlled anodic dissolution at atomic level of the electrically conductive work-piece by a desired shaped tool due to flow of high current at relatively low potential difference through an electrolyte which is quite often water based neutral salt solution. ECM is one of advanced machining technologies and has been applied in highly specialized fields, such as aerospace, aeronautics, defense and medical industries. In present days, ECM is used in other industries such as automobile and turbo-machinery because of its various advantages. In case of complicated shapes of work-piece it is very difficult to know the machining variables distribution within the inter electrode gap (IEG). By studying the flow pattern of electrolyte, we can predict the machining variable distribution accurately and thus can avoid the passivation which is the major problem in ECM in complicated shape cases. Again, two phase effect (hydrogen bubble generation) has a major role on the machining variables as well as on the material removal rate and surface roughness. The flowing electrolyte collects the evolving hydrogen gas generated at the cathode. Electrolyte has three main functions in ECM. It carries the current between the tool and work piece, it removes the products of the reaction from the cutting region, and it removes heat produced in operation. Normal electrolyte used for ECM for all common metals & alloys is solution of Sodium Chloride (NaCl) in water. They react with the work piece and form a salt which dissolves in electrolyte.

II. EXPERIMENTATION

This deals with the experiment that has been conducted in the ECM set up. The experiments were conducted with L-shaped tool as per the dimensions of model to find out the MRR to validate the simulation results.

2.1. ECM Set up

The ECM set up used for the experiment is as shown in the fig.2.1 and the control panel is as shown in fig.2.2.

Fig.2.1: ECM set up used for the experiment

https://dx.doi.org/10.22161/ijaers/310.22 *ISSN: 2349-6495(P) | 2456-1908(O)*

Fig.2.2: Control panel

2.2. Fabrication of Tool and Work-Piece

For doing the experiment, we need to fabricate the tool and work-piece of exact dimension as that in the modelling. For fabricating the tool, we have procured a copper rod and cut the rod into L-shape is produced by facing, filing and turning operation was done and to polish it, we have used grinding operation. Again, for the groove, a through hole is drilled on the tool by the help of the drilling machine. Now, the L-shape is ready. A pipe having one side threaded end is used for connecting the tool with the tool holder. The pipe is fabricated with a through hole of same dimension as that of the groove in the tool. After generation of L-shape and the pipe, both of them are aligned properly and brazed as shown in the fig.2.3. After brazing, the required tool is ready the bottom of tool is shown in fig.2.4. The work-piece material used is iron which is procured and is cut in to 9 circular pieces of diameter 60 mm.

Fig. 2.3: Brazing of tool

Fig. 2.4: Bottom of tool

2.3. Taguchi Experimental Design and Analysis

Taguchi design focused at greater understanding of variations of parameters. Taguchi proposed to extend each experiment with an "outer array" called the orthogonal array. In this experiment, Minitab software is used for Taguchi design. In this study, 3 level designs (3 factors) with total of 9 numbers of experiments are conducted and for this orthogonal array L9 is used. The machining parameters and their levels with details are shown in table 2.1. The experimental observations for tool are shown in the table 2.2. The iron work-pieces after machining for all the runs using tool is shown in fig.2.5.

Table.2.1: Machining parameters and their levels

Machining parameters	Symbol	Unit	Levels		
			Level1	Level2	Level 3
Voltage	V	V	10	12.5	15
Flow rate	F	m/s	30	35	40
Concentration	C	g/L	60	85	110

Table.2.2: Experimental observation table using L9 orthogonal array

Run	1	2	3	4	5	6	7	8	9
Voltage (V)	10	10	10	12.5	12.5	12.5	15	15	15
Flow rate (m/s)	30	35	40	30	35	40	30	35	40
Concentration(g/L)	60	85	110	85	110	60	110	60	85
Initial weight (g)	419	379	418	538	454	455	413	414	514
Final weight (g)	418	377	416	535	452	454	411	413	512
Time (min)	10	10	5	10	10	5	10	10	5
MRR (mm^3/min)	12.7	25.4	50.9	38.2	25.4	25.4	25.4	12.7	50.9

Fig.2.5: Work-pieces after machining

III. MODELLING AND SIMULATION

The analysis techniques, geometric modeling and boundary conditions are explained in this work. ECM set up consists of a work-piece, tool and an electrolyte solution. Work-piece should be electrically conducting material and the tool may or may not be. Commonly used electrolytes are NaCl solution and NaNO3. To get required shape in the work-piece, tool should be designed properly. The shape of the tool affects the critical parameters of machining. Another important aspect in the modelling of ECM is the flow

https://dx.doi.org/10.22161/ijaers/310.22 *ISSN: 2349-6495(P) | 2456-1908(O)*

pattern of electrolyte and the various intervening factors those are affected by the two phase flow pattern of electrolyte.

3.1. Geometrical Modelling

A finite element based commercial CFD software package ANSYS is used under the Windows7 64-bit operating system for the simulation study. In the present simulation process, the modelling is done with ANSYS software. The L-shaped tool with central through hole model is used for the simulation study. The initial shape of the work-piece is circular in shape with 60 mm diameter and 20 mm height. Model of work-piece is shown in fig 3.1. Electrolyte used for this simulation is NaCl solution (20%). The electrolyte starts flowing with a constant diameter of 3 mm from the inlet of the tool. The long side of the L-shape is having 30 mm length and short side of 15 mm length and the central hole has diameter of 3mm. Top view of the tool is shown in fig 3.2 and 3D view is shown in fig 3.3. Inter electrode gap (IEG) is kept constant at 0.5 mm. The key dimensional feature of the physical model is as shown in table 3.1. The complete physical model of workpiece tool set up is as shown in fig. 3.4.

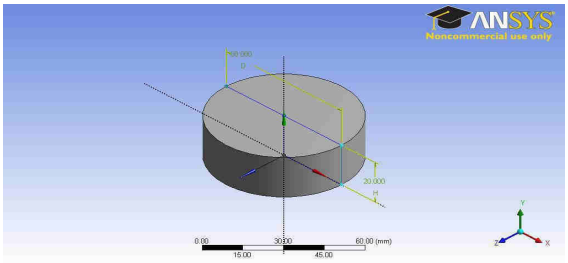

Fig. 3.1: Work-piece used for simulation

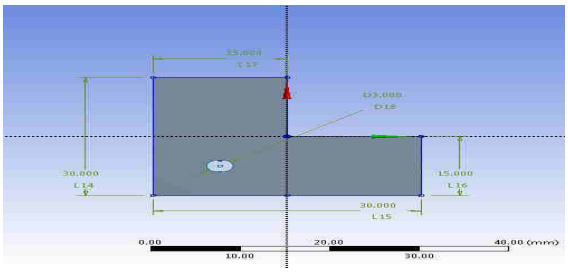

Fig. 3.2: Top view of tool used for simulation

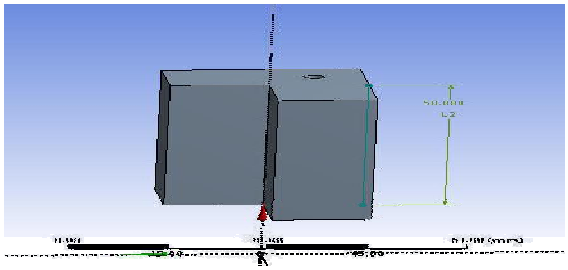

Fig. 3.3: 3D view of tool used for simulation

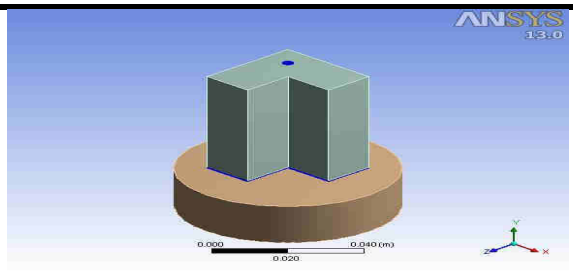

Fig. 3.4: Physical model

Table.3.1: Element type

S.No	Component	Materia	Physical state	Shape	Dimension(mm)
1	Work-piece	Iron	Solid	Cylindrical	60 dia. X 20 ht.
2	Tool	Copper	Solid	L-shaped	Arm 30 X Width 15 X Height 50 X central hole 3Ø
3	Medium	Brine	Fluid	-	-

3.2. L Shaped Tool with Central Through Hole

A simple L shaped tool having a central through hole with a diameter of 3mm and height of 50 mm. This centre of the hole is fixed on (-7.5,-7.5) coordinate in the XZ plane. Fluid is flowing through the through hole and flow out through the IEG. Top view of the tool is shown in fig.3.2 and 3D view is shown in fig 3.3. Inter electrode gap (IEG) is kept constant is 0.5mm.

3.2. Boundary Conditions

Before considering the boundary conditions, the computational domains should be specified. In this simulation three domains are being used such as two solid domains and a fluid domain. One solid domain for work-piece and other is for tool. Materials of solid domain are considered as pure solids. Morphology of materials in the solid domain is given as continuous solid and reference temperature is given 298K. Electric potential model with automatic value is chosen from Electromagnetic model. Fluid domain is constructed for electrolyte. Two materials are taken for fluid domain as it is a two phase flow analysis. Morphology for fluid domain is taken as continuous fluid for brine and dispersed fluid for hydrogen bubbles. The properties of the materials used in these domains are set as per the values in the table 3.2.

Table.3.2: Material properties

Properties	**Brine**	**Copper**	**Iron**	**Air**
Molar mass (kg/kmol)	58.44	63.55	55.85	-
Density (kg/m^3)	1050	8933	7860	-

https://dx.doi.org/10.22161/ijaers/310.22 *ISSN: 2349-6495(P) | 2456-1908(O)*

Specific heat (J/kg K)	3760	385	460	-
Dynamic viscosity (Pa s)	0.001	-	-	-
Thermal conductivity (W/m K)	0.6	401	80	-
Electrical conductivity (S/m)	8.43	5.96E+07	1E+07	-
Convection coefficient ($W/m^2 K$)	1000	-	-	100

IV. RESULTS AND DISSCUSSIONS

The analysis of the results and discussion of the model generated in ANSYS as per the required dimentions. It shows the crucial parameters affecting overall machining process of ECM in terms of contours from which we can predict the variation of these parameters in the IEG and their effects.

4.1. Volume Fraction Profile

Fig.4.1 shows the volume fraction profiles of the tool generated. The inlet velocity for this simulation study was taken as 40 m/s. The volume fraction contour has shown the volume fraction of brine in the homogenous mixture of continuous fluid brine and a dispersed fluid hydrogen bubble.

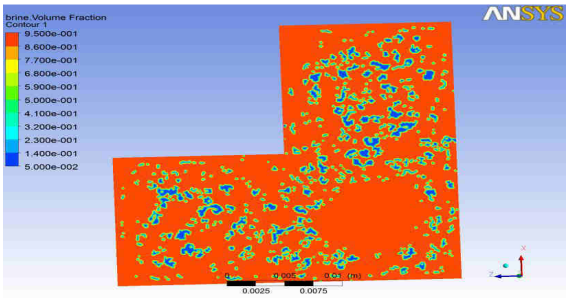

Fig.4.1: Volume fraction profile for tool

4.2. Velocity Profile

Fig.4.2 shows the velocity profile for tool with an inlet velocity of 40 m/s, which indicates that velocity of two phase electrolyte is increased from the groove to the boundary partly due to reduction in area of flow and partly due to formation of hydrogen bubbles resulting in more turbulence.

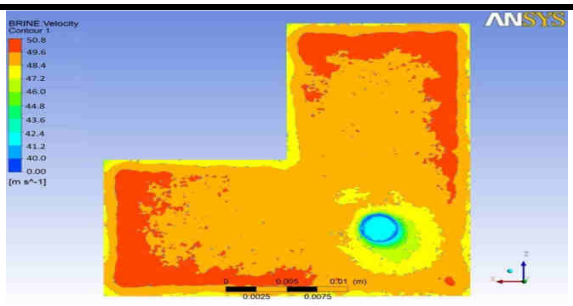

Fig.4.2: Velocity profile for tool

4.3. Pressure Profile

The pressure profiles describe about the variation in pressure in the IEG on the plane of machining area. As in this tool, there is very large amount of production of hydrogen bubbles and because of cavitation effect, the pressure increases at a large number of nucleus sites from the groove outlet towards the outer boundaries showing the places of hydrogen bubbles and hence high pressure zones as shown in fig. 4.3.

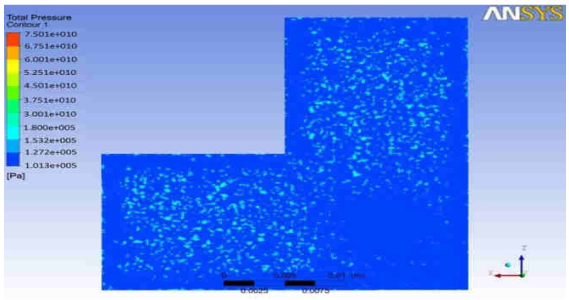

Fig.4.3: Pressure profile for tool

4.4. Temperature Profile

Temperature pattern is a very crucial aspect for this study. As can be shown in the fig.4.4, the temperature is least at the groove outlet and goes on increasing rapidly as we move to outside for tool. It crosses the boiling point of brine which in turn produces phase change and production of hydrogen bubbles as secondary dispersed phase.

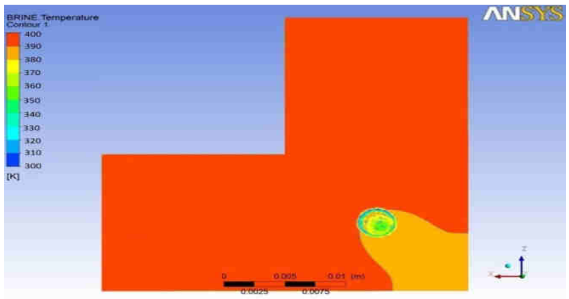

Fig.4.4: Temperature pattern for tool

4.5. Heat Flux Pattern

Heat is generated in the IEG due to joule's heating. By appropriately designing tool shape, the heat generated and

https://dx.doi.org/10.22161/ijaers/310.22 *ISSN: 2349-6495(P) | 2456-1908(O)*

thus the overheating can be avoided. The fig.4.5, describe the heat flux pattern for the tool model.

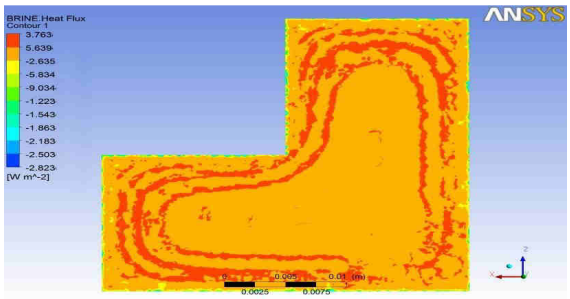

Fig.4.5: Heat flux contour for tool

In this simulation, we have assumed that the heat generated in the IEG is only due to Joule's heating. Heat flux is nothing but the heat generated per unit machining area. For tool, the value is less near the groove outlet. But as we proceed towards the outer, the heat flux increases to a very high amount. This higher value of heat flux exists all over the outer boundary of L-shape in a comparatively larger area. The minimum amount of heat flux is -2.823 W/m^2 and maximum amount is 3.763 W/m^2.

4.6. Interphase Mass Transfer Profile

Fig.4.6 shows the interphase mass transfer profile for tool. Interphase mass transfer rate depicts the conversion of secondary phase from primary one. It may occur due to bubbling of brine and hence production of hydrogen bubbles. In this larger amount of conversion from brine to hydrogen and this conversion goes on increasing from the groove outlet towards the outer boundaries. This conversion can be described as nucleus sites formed randomly throughout the L-shape except at the groove outlet.

4.7. Turbulent Kinetic Energy Profile

Fig.4.7 shows the turbulent kinetic energy contour for tool. As in this analysis, we have considered k-ϵ model for the turbulence, so there is a variation in k as well as in ϵ for a variation in the turbulence. Turbulence in the k- ε model depends on turbulent kinetic energy (k) and turbulent eddy dissipation (ε). Roughness of the machined surface has a direct link with the turbulence. Turbulent kinetic energy depicts the energy in the turbulence. Turbulent kinetic energy is produced by fluid shear, friction or buoyancy or through external forces at low frequency eddy scale. For this tool the turbulent kinetic energy value is lower near the groove outlet and increases towards the outer boundaries because of more turbulence which may be due to the formation of hydrogen bubbles. The minimum turbulent kinetic energy is 1.493 X 10^{-1} m^2/s^2 near the groove whereas maximum value is 5.617 X 10^9 m^2/s^2 near the outer portions as depicted from the fig.4.7.

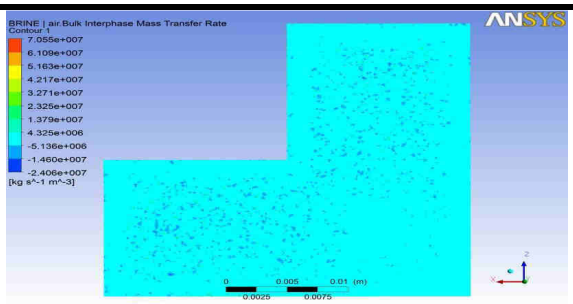

Fig.4.6: Interphase mass transfer profile for tool

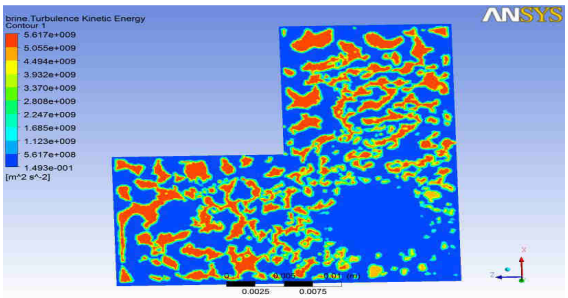

Fig. 4.7: Turbulent kinetic energy contour for tool

V. CONCLUSION

Three dimensional two phase flow pattern analysis of electrochemical machining with L-shaped tool provides fundamental idea of velocity distribution, pressure pattern, temperature profile, turbulence etc. in the IEG. A cylindrical Iron work-piece, L-shaped Copper tool and 20% brine solution as electrolyte was considered in this analysis. The tool is analysed with inlet velocity of 40 m/s and with a residual target of 1x10-4. To validate the simulated result, experimentation was carried out in ECM by fabricating the tool Model with the same dimension as in simulation. The experimental results are analysed by using CFD software. Volume fraction profile for brine indicates that more hydrogen bubbles are generated and the velocity profile indicate very high value at the outer side of groove due to the turbulence created because of the generation of hydrogen bubbles. Pressure profile describes the pressure in the machining area and it has randomly generated high pressure spots throughout the machining area except at groove outlet because of the cavitation effect at the points of hydrogen bubbles generation. Similarly, temperature pattern indicates boiling effect in the machining area resulting in the generation of hydrogen bubbles.

REFERENCES

[1] Tsuboi, R. and Yamamoto, M. (2009) Modeling and applications of electrochemical machining process. *Proceedings of the ASME International Mechanical*

Engineering Congress & Exposition IMECE, November 13-19, Lake Buena Vista, Florida, USA.

[2] Bilgi, D.S., Kumar, R., Jain, V.K. and Shekhar, R. (2008) Predicting radial overcut in deep holes drilled by shaped tube electrochemical machining. *International journal of advanced manufacturing technology*, Vol. 39, pp. 47-54.

[3] Neto, J., Silva, E. and Silva, M. (2006) Intervening variables in electrochemical machining. *Journal of Materials Processing Technology*, Vol. 289, pp. 92-96.

[4] Mukherjee, S.K., Kumar, S., Srivastava, P.K. and Kumar, A. (2008) Effect of valency on material removal rate in electrochemical machining of aluminium. *Journal of materials processing technology*, Vol. 202, pp. 398-401.

[5] T.Haisch, E.Mittemeijer, J.W.Schultze Electrochemical machining of the steel 100Cr6 in aqueous NaCl and NaNO3 solutions: microstructure of surface films formed by carbides, Electrochimica Acta 47 (2001) 235–241.

[6] Conner, M.E., Baglietto, E. and Elmahdi, A.M. (2010) CFD methodology and validation for single-phase flow in PWR fuel assemblies. Nuclear Engineering and Design, Vol. 240, pp. 2088–2095.

[7] Frank, T., Zwart, P.J., Krepper, E., Prasser, H.M. and Lucas, D. (2008) Validation of CFD models for mono- and polydisperse air–water two-phase flows in pipes. Nuclear Engineering and Design, Vol. 238, pp. 647–659.

[8] Li, X.G., Liu, D.X., Xu, S.M. and Li, H. (2009) CFD simulation of hydrodynamics of valve tray. Chemical Engineering and Processing, Vol. 48, pp. 145–151.